

# INTERNATIONAL SOCIETY FOR SOIL MECHANICS AND GEOTECHNICAL ENGINEERING



*This paper was downloaded from the Online Library of the International Society for Soil Mechanics and Geotechnical Engineering (ISSMGE). The library is available here:*

<https://www.issmge.org/publications/online-library>

*This is an open-access database that archives thousands of papers published under the Auspices of the ISSMGE and maintained by the Innovation and Development Committee of ISSMGE.*

# Influence of superstructure on behaviour of model piled rafts in sand under shaking tests

## Influence de superstructure sur le comportement des modèles de radeau empilé en sable aux essais tremblants

T. Matsumoto, K. Fukumura & A. Oki  
 Graduate School of Natural Science, Kanazawa University, Kanazawa, Japan

### ABSTRACT

A series of seismic load tests were carried out on model piled rafts in dry sand by using a shaking table. In the test series, the height of the gravity centre of superstructure on the raft was varied while keeping the mass of the superstructure constant, in order to investigate the influence of the height of the gravity centre of the superstructure on the behaviour of the piled raft foundation. Furthermore, a series of static horizontal load tests on the same model piled rafts were conducted, in which the vertical level of the loading point was set at the height of the gravity centre of superstructure. The results from both tests are presented and discussed.

### RÉSUMÉ

Une série d'essai séismique de charge a été agie sur le modèle de radeau empilé qui est situé dans le sable sec au moyen d'une table de secousse. Pendant les expériences, l'altitude du centre de la gravité de la superstructure sur le radeau a été ajustée différemment tandis que la masse de la superstructure était gardée constante afin d'étudier l'influence de l'altitude du centre de la gravité de la superstructure sur le comportement de la base de radeau empilée. En outre, une série d'essai de charge horizontale statique sur le même modèle de radeau empilé a été conduite tandis que la ligne de charge verticale était fixe au centre de la gravité de la superstructure. Les résultats des deux essais sont présentés et discutés.

### 1 INTRODUCTION

Piled raft foundations have been widely recognized as an economical and rational type of pile foundations when they are subjected to vertical loading (e.g., Poulos & Davis, 1980; Randolph, 1994; Horikoshi & Randolph, 1999; Katzenbach & Moorman, 2001).

In highly seismic areas such as Japan, estimation of the behaviour of pile groups and piled rafts subjected to horizontal loading or seismic loading is an important issue in seismic design of pile foundations. Behaviour of model piled rafts and model pile groups subjected to static or seismic horizontal loads have been intensively investigated in 1-g field model tests (Pastsakorn *et al.*, 2002; Fukumura *et al.*, 2003) and in centrifuge modelling (Horikoshi *et al.*, 2003a; Horikoshi *et al.*, 2003b). These test results show that piled rafts are also economical and rational foundations even for horizontal loading.

However, in the experimental research mentioned above, the influence of the superstructure on the behaviour of piled raft models was not explicitly considered. In actual structures such as bridge structure, superstructure including abutment or pier as well as bridge girder exists on the raft, making its height of the gravity centre higher compared to the raft breadth.

Hence, in this paper, the influence of the height of the gravity centre of superstructure on the behaviour of model piled rafts was investigated by conducting shaking table tests and static horizontal load tests on model piled rafts of the same mass having different heights of the gravity centres.

### 2 SIMILARITY RULE FOR 1-G FIELD MODEL TEST

It is important to consider the similarity rule to deduce the behaviour of a prototype structure from the behaviour of the corresponding model.

Dry Toyoura sand having a relative density,  $D_r$ , of 95% was used for the model ground throughout. The physical properties of Toyoura sand are summarized in Table 1. A series of triaxial

consolidated drained shear tests (CD test) was conducted to obtain the stress dependency of the shear modulus,  $G$ . The tests were carried out with soil specimens of  $D_r = 90$  to 95 %, 100 mm high and 50 mm radius, with different confining pressures,  $p_0$ , of 50, 100, 200 and 300 kPa.

From initial linear part of the measured deviator stress,  $q$ , versus axial strain,  $\epsilon_a$ , of each test, the shear modulus was estimated as  $G = q/(\epsilon_a - \epsilon_r)$  where  $\epsilon_r$  is the radial strain and is plotted against the confining pressure,  $p_0$ , in Fig. 1. The measured values of  $G$  are fitted by the line in Fig. 1, which is expressed as

$$G = G_{\text{ref}} (p_0 / p_{\text{ref}})^{0.5} \quad (1)$$

where  $p_{\text{ref}}$  is a reference value of confining pressure (=100 kPa) and  $G_{\text{ref}}$  (=29163 kPa) is the value of  $G$  at  $p_0 = p_{\text{ref}}$ .

Table 1. Physical properties of Toyoura sand.

Density at test	$\rho_t$	1.635 t/m <sup>3</sup>
Relative density at test	$D_r$	95 %
Internal friction angle	$\phi'$	44 deg.
Mean grain size	$D_{50}$	0.162 mm
Density of soil particle	$\rho_s$	2.661 t/m <sup>3</sup>
Maximum density	$\rho_{\text{dmax}}$	1.654 t/m <sup>3</sup>
Minimum density	$\rho_{\text{dmin}}$	1.349 t/m <sup>3</sup>

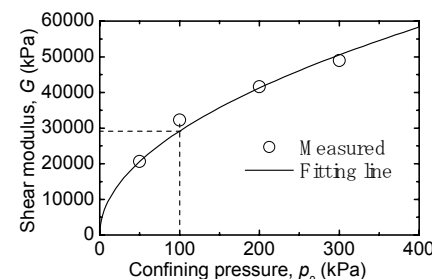


Figure 1. Shear modulus versus confining pressure.

The shear modulus of the sand is proportional to the square root of  $p_0$ . Hence, the similarity rule for model tests at 1-g field proposed by Iai (1989) can be applied to the model tests.

### 3 TEST APPARATUS AND TEST PROCEDURE

#### 3.1 Model piled raft and model superstructure

Figure 2 shows the model raft and the model pile. The square model raft, with a breadth of 80 mm, was made of an aluminum plate with a thickness of 25 mm. The mass of the model raft was 0.4 kg. In order to increase the friction at the raft base, the base was roughened. The interface frictional angle between the raft base and the model ground was 30.5 degrees, i.e., the coefficient of frictional angle was 0.59.

Aluminum pipes with an outer diameter of 10 mm, an inner diameter of 8 mm and a length of 170 mm were used for the model piles. Each pile toe was capped with a thin aluminum plate. Young's modulus,  $E_p$ , and Poisson's ratio,  $\nu_p$ , were determined from bending tests of the model piles. Each pile was instrumented with foil strain gauges along the pile shaft as shown in Fig. 2(b) in order to obtain the distributions of the axial forces, the shear forces and the bending moments of the pile. The geometrical and mechanical properties of the model pile are listed in Table 2, together with the properties of a corresponding prototype pile when the scaling factor,  $\lambda$ , is taken as 50.

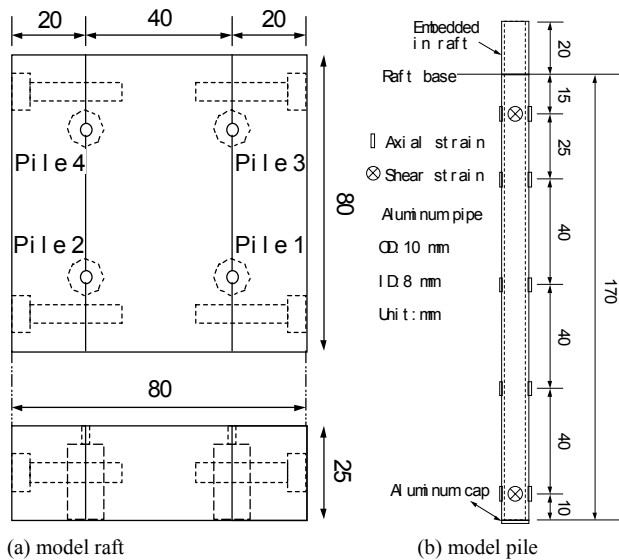


Figure 2. Model piled raft.

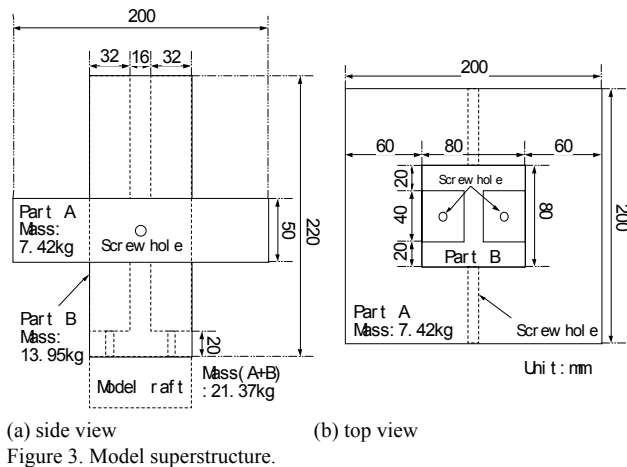


Figure 3. Model superstructure.

Four model piles were connected to the model raft with a pile spacing of 40 mm. The head of each pile was rigidly connected to the raft. Note that configuration of the model piled raft is the same as was used in the centrifuge tests by Horikoshi *et al.* (2003a, 2003b).

Fig. 3 shows the model superstructure that was attached on the model raft. The model superstructure consists of two parts. Part A with a mass of 7.42 kg can slide vertically along Part B having a mass of 13.95 kg so that the height of the gravity centre of the model superstructure can be changed. Note that the bending rigidity of Part B is so large that its bending deformation is negligible. A circular plate with a mass of 22 kg was also prepared for model superstructure with a low gravity centre (see Fig. 4).

Table 2. Geometrical and mechanical properties of the model pile.

	Model	Prototype ( $\lambda=50$ )
Outer diameter, $r_o$ (mm)	10	500
Wall thickness, $t_w$ (mm)	1	50
Length, $L$ (mm)	170	8500
Cross section area, $A$ (mm <sup>2</sup> )	28.3	70685.8
Young's modulus, $E_p$ (GPa)	67.1	3354
Poisson's ratio, $\nu_p$	0.345	0.345
Longitudinal rigidity, $E_p A$ (GN)	$1.90 \times 10^{-3}$	33.53
Bending rigidity, $E_p I$ (GNm <sup>2</sup> )	$19.4 \times 10^{-8}$	0.859

#### 3.2 Test set-up and test procedure

Fig. 4 shows an illustration of the final stage of the test set-up just before starting a dynamic (seismic) load test in the case of the low gravity centre superstructure. The model foundation was set near the centre location of a laminar box with a special rig before making the model ground. The laminar box with dimensions of 210 mm in width, 560 mm in length and 310 mm in depth was consisted of 16 layers of aluminum frames with a thickness of 20 mm. Dry Toyoura sand was poured in the laminar box and compacted to  $D_r = 95\%$  by applying small vibrations using the shaking table. After the completion of the preparation of the model ground, a model superstructure was bolted on the top of the raft.

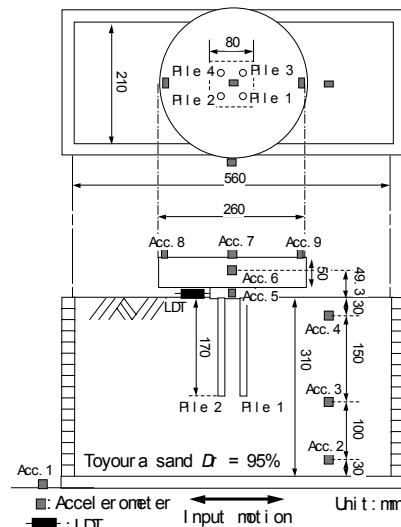


Figure 4. Test set-up for seismic load test.

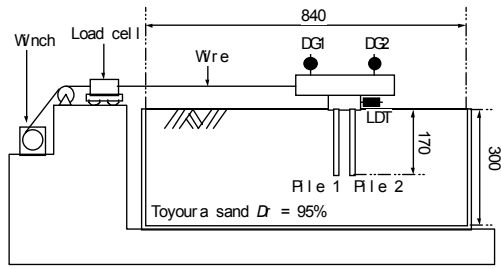


Figure 5. Test set-up for static horizontal load test.

Accelerometers were embedded in the model ground (Acc. 2, to 4) and attached to the side of the model raft (Acc. 5), and the side and the top of the model superstructure (Acc. 6 to 9). An accelerometer (Acc. 1) was placed on the shaking table to measure the input acceleration.

A series of seismic tests was carried out with target amplitude of 100 gal. Sinusoidal input waves of the frequencies from 5 to 95 Hz at an interval of 5 Hz were applied.

Horizontal static load tests were also carried out using the model ground prepared in a rigid acrylic box with dimensions of 500 mm in width, 840 mm in length and 300 mm in depth (Fig. 5). The horizontal load was applied at the level of the gravity centre of the superstructure by pulling the superstructure by means of a winch and a wire at a slow displacement rate less than 1 mm/min. The horizontal displacement of the raft was measured by a laser displacement transducer (LDT), and the vertical displacements of the superstructure were measured at two points by dial gauges (DG) to obtain the inclination of the superstructure.

#### 4 TEST RESULTS

Behaviour of the model pile rafts with the gravity centre heights of 49.3 mm (low gravity centre) and 123.4 mm (middle gravity centre) from the ground level, respectively, are presented and compared in this paper. Test name and test conditions are summarised in Table 3. The proportion of vertical load carried by the piles before starting load test is also shown in Table 3. The vertical load proportions were similar in all of these tests.

The transfer functions obtained from dynamic (seismic) load tests, DRL and DRM, are shown in Fig. 6. The response factor is defined as the ratio of the response horizontal acceleration to the input horizontal acceleration.

Table 3. Test name and test conditions.

Test name	Height of gravity centre from G.L.	Type of loading	Proportion of vertical load carried by piles before load test (%)
DRL	Low (49.3mm)	Dynamic	72.6
DRM	Middle (123.4mm)	Dynamic	73.4
SRL	Low (49.3mm)	Static	79.6
SRM	Middle (123.4mm)	Static	78.5

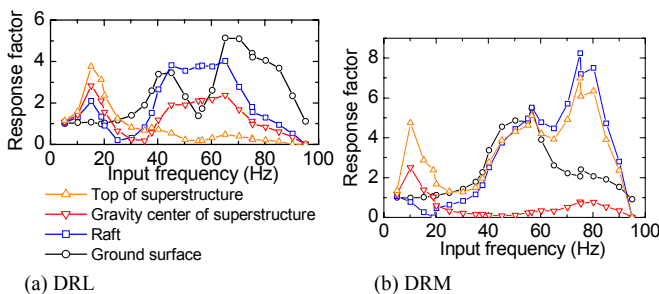


Figure 6. Transfer function of horizontal acceleration.

The response factors at the top and the gravity centre of the superstructure, the raft and the ground surface (Acc. 4) are indicated in Fig. 6. The peak response factor of the gravity centre was obtained at the input frequency of 15 Hz in DRL, while that in DRM was obtained at 10 Hz indicating the influence of higher level of the gravity centre of the superstructure. At input frequency of 5 Hz, the response factors observed in both DRL and DRM were the almost same as 1.

Hereafter, the behaviours of the model piled rafts at the input frequency of 5 Hz in DRL and DRM are compared to demonstrate the influence of the height of the gravity centre of the superstructure.

Figure 7 shows the input accelerations in DRL and DRM. Fig. 8 shows the input acceleration (Acc 1) and the response horizontal acceleration (Acc 6) at the height of the gravity centre during a cycle of loading indicated by the shaded area in Fig. 7. It is seen that there is no time shift between the input and the response acceleration in both DRL and DRM, but the response factor is a little bit of larger in DRM compared to DRL.

The relationships between the horizontal load and the horizontal displacement of the raft measured by LDT (see Fig. 4) obtained from seismic load tests (DRL & DRM) and static horizontal load test (SRL & SRM) are shown in Fig. 9. The total horizontal load in seismic test was calculated as the product of the acceleration measured at the gravity centre and the mass of the superstructure. The pile load is the sum of the shear forces measured at the pile heads of 4 piles. The difference between the total load and the pile load is the horizontal load carried by the raft base. It can be seen from Fig. 9 that the raft base resistance is effectively mobilized during both dynamic and static loading tests. Contribution of the raft base resistance is pronounced in the case of the superstructure with the middle gravity centre height compared to the low gravity centre height. The horizontal stiffness of the model foundation in DRL and SRL is almost equal, while the horizontal stiffness in DRM is higher than that in SRM.

Fig. 10 shows the relationship between the inclination and the horizontal displacement of the raft obtained from the seismic load tests and the static load tests. The inclination becomes larger as the height of the gravity centre of the superstructure becomes larger in both seismic and static load tests. The results from the seismic and the static tests are comparable.

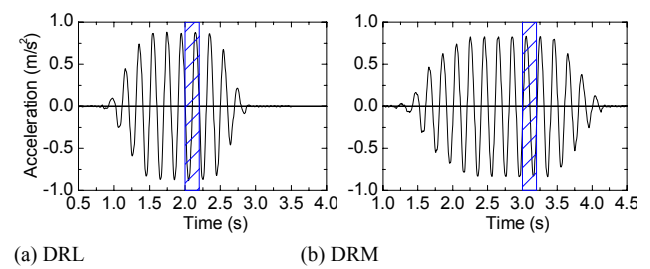


Figure 7. Input acceleration.

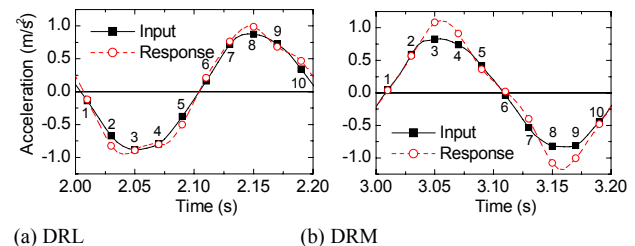


Figure 8. Response horizontal acceleration at the gravity centre.

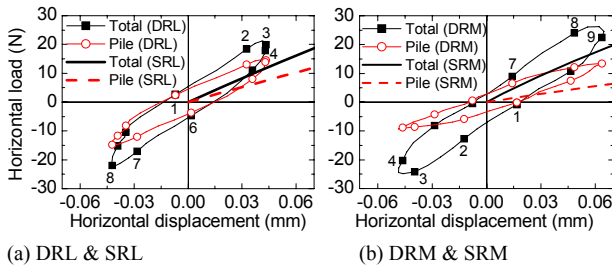


Figure 9. Horizontal load versus horizontal displacement of raft.

The shear forces near the pile head and the pile tip when the total horizontal load of 20 N was applied to the superstructure are shown in Fig. 11.

Note that the horizontal load of 20 N is the maximum horizontal load generated in the seismic load test on the low gravity centre superstructure (see DRL in Fig. 9(a)). On the whole, the shear force near the head of pile 1 (front pile at this time moment) is larger than that of pile 2 (back pile at this time moment). For the positions of piles 1 and 2, refer to Fig. 4. Distributions of the shear forces of the piles in DRL are very similar to those in SRL (Fig. 11(a)), while the shear force near the head of pile 1 in DRM is much larger than that in SRM (Fig. 11(b)).

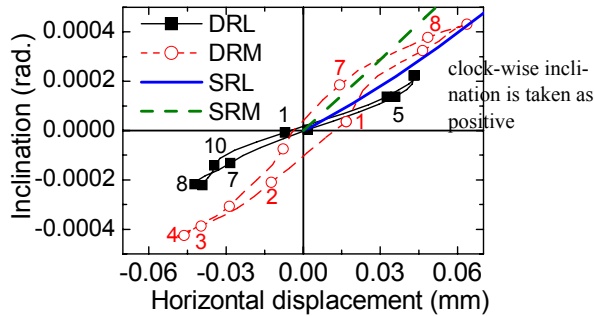


Figure 10. Inclination versus horizontal displacement of raft.

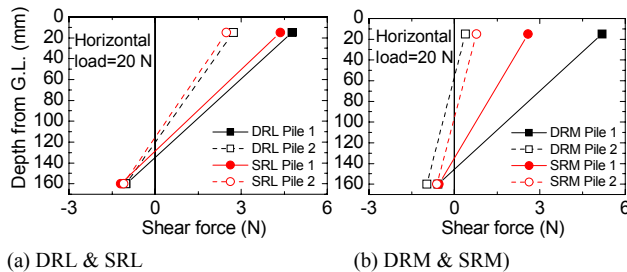


Figure 11. Distribution of shear forces in piles.

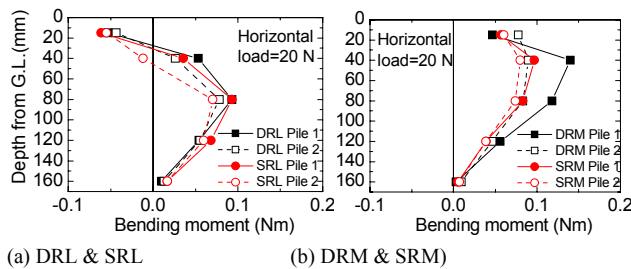


Figure 12. Distribution of bending moments in piles.

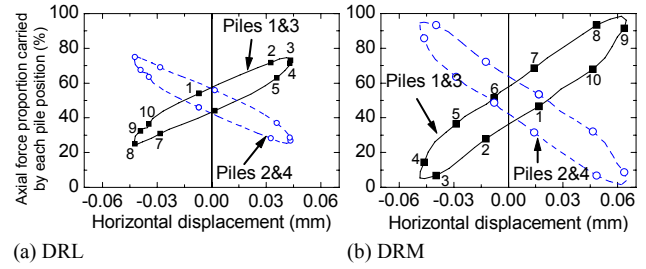


Figure 13. Proportions of vertical load carried by each pile.

The distributions of bending moments in the piles are compared in Fig. 12 for the horizontal load of 20 N. The distributions of bending moments in the front and back piles are similar between DRL and SRL, and there is no distinction of the pile bending moments between the dynamic loading and the static loading (Fig. 12(a)). Distributions of the bending moments of the front and back piles are similar in case of SRM, while larger bending moments are generated in the front pile in DRM (Fig. 12(b)).

The behaviours of the piles indicated in Fig. 11 and Fig. 12 are related to the inclination of the raft (Fig. 10) and the proportions of the vertical loads carried by the front piles (piles 1 and 3) and the back piles (piles 2 and 4) shown in Fig. 13. When the raft inclines in the clock-wise direction, the axial forces at the heads of the front piles increase and those of the back piles decrease almost linearly with the increase in the inclination of the raft. It is noted that this behaviour is pronounced in DLM (Fig. 13(b)). The increase in the vertical load in the front piles may indicate the increase in the contact pressure between the raft base and the ground surface near the front piles. This increase in the contact pressure leads to the increase in the stresses in the soils around the front piles, resulting in the increase in the strength and the rigidity of the sand soils. Hence, the lateral resistance of the front piles is increased, and thereby the shear forces and bending moments in the front piles become larger than those in the back piles. This phenomena is also observed in centrifuge modelling by Horikoshi *et al.* (2003b).

## 5 CONCLUSIONS

A series of seismic and static horizontal load tests on the model piled rafts having superstructures of the same mass with different heights of the gravity centre were conducted at 1-g field. The following conclusions were derived:

- 1) The resonant frequency is decreased as the height of the gravity centre of the superstructure is increased, as expected.
- 2) At a low input frequency, the behaviour of the model piled raft having a superstructure of low gravity centre under seismic loading is similar to the behaviour of the model piled raft subjected to static horizontal loading.
- 3) Even if the horizontal response accelerations of the gravity centres of the superstructures are the same, the inclination of the raft, the shear forces and the bending moments of the piles are increased as the height of the gravity centre of the superstructure is increased.
- 4) The above results demonstrate the importance of consideration of the height of the gravity centre of a superstructure in seismic design of piled raft foundation.

The authors thank Dr. K. Horikoshi and Mr. T. Watanabe of Taisei Corporation and Dr. P. Kitiyodom of Kanazawa University for their valuable suggestions and discussions.

## REFERENCES

- Iai, S. 1989. Similitude for shaking table tests on soil-structure-fluid model in 1g gravitational field, *Soil and Foundations*, **29**(1), 105-118.
- Fukumura, K., Matsumoto, T., Ohno, A. and Hashizume, Y. 2003. Experimental study on behavior of piled raft foundations in sand using shaking table at 1-g gravitational field. *Proc. BGA Int. Conf. on Foundations: Innovations, observations, design & practice*, 307-320.
- Horikoshi, K., Matsumoto, T., Hashizume, Y., Watanabe, T. and Fukuyama, H. 2003a. Performance of piled raft foundations subjected to static horizontal loads. *Inter. Jour. of Physical Modelling in Geomech.*, **3**(2), 37-50.
- Horikoshi, K., Matsumoto, T., Hashizume, Y., and Watanabe, T. 2003b. Performance of piled raft foundations subjected to dynamic loading. *Inter. Jour. of Physical Modelling in Geomech.*, **3**(2), 51-62.
- Horikoshi, K. and Randolph, M. F. 1999. Estimation of overall settlement of piled rafts, *Soils and Foundations*, **39**(2), 59-68.
- Katzenbach, R. and Moormann, C. 2001. Recommendations for the design and construction of piled rafts, *Proc. 15<sup>th</sup> ICSMGE*, **2**, 927-930.
- Pastsakorn, K., Hashizume, Y. and Matsumoto, T. 2002. Lateral load tests on model pile groups and piled raft foundations in sand. *Proc. Int. Conf. on Physical Modelling in Geotech.*, St. John's, 709-714.
- Poulos, H. G. and Davis, E. H. 1980. *Pile Foundation Analysis and Design*, John Wiley and Sons, New York.
- Randolph, M. F. (1994): Design methods for pile groups and piled rafts, *Proc. 13<sup>th</sup> ICSMFE* 1994, New Delhi; **2**, 61-546.